

Interaction of magnesium or zinc with aminodinitroethylenes – DFT treatment

Lemi Türker

Department of Chemistry, Middle East Technical University, Üniversiteler, Eskişehir Yolu No: 1, 06800 Çankaya/Ankara, Turkey
e-mail: lturker@gmail.com; lturker@metu.edu.tr

Abstract

Aminodinitroethylenes are pull-push type structures isoconjugate with alternant hydrocarbon anions. They constitute substructures of various potent explosive molecules. Presently, aminodinitroethylenes and their magnesium and zinc composites have been investigated thoroughly within the constraints of density functional theory at the level of B3LYP/6-31++G(d,p). The collected data have revealed that the optimized structures of them have exothermic heats of formation and favorable Gibbs free energy of formation values. They are thermally favored and electronically stable at the standard states. Various structural and quantum chemical data have been collected and discussed, including UV-VIS spectra. The data reveal that in the composites some electron population transfers from the inorganic to the organic components occur so that the zinc atom causes the rupture of N-H bond of structure-A.

1. Introduction

Aminodinitroethylenes which possess push-pull type character and in embedded form, are the main backbone of some explosive materials such as in FOX-7 (1,1 -diamino-2,2-dinitroethylene) structure [1,2] or in some dyes as it is or its heteroanalogs [3].

Push-pull type double bonds have long been a subject of interest and study for various purposes such as conformational analysis, nuclear magnetic resonance, non-covalent interactions, solvent effects, etc [4-15]. It is known that the diminution of the C=C rotational barrier in push-pull type ethylenes is a consequence of electronic/resonance effects, steric interactions between the donor and acceptor groups, or a combination of both of these [4-6].

Amino and nitro groups have donor and acceptor properties, respectively in terms of classical resonance theory. When they are attached to a double or a triple bond, a polar system may arise depending on the positions of the donor and acceptor groups.

Non-covalent interactions can be classified into different categories, such as electrostatic, π -effects, van der Waals forces, and hydrophobic effects [4,9-16]. Ion-dipole and dipole-dipole interactions depend on the orientations of the dipole. Dipole-induced dipole interactions are important even between molecules with permanent dipoles.

2. Method of Calculations

In the present study, all the initial optimizations of the structures leading to energy minima have been achieved first by using MM2 method which is then followed by semi empirical PM3 self consistent fields

Received: February 26, 2026; Accepted: March 21, 2026; Published online: March 23, 2026

Keywords and phrases: aminodinitroethylenes, push pull, explosive, DFT calculations, UV-VIS spectra.

molecular orbital method [17-19]. Afterwards, the structure optimizations have been achieved within the framework of Hartree-Fock and finally by using density functional theory (DFT) at the level of B3LYP/6-31++G(d,p) [20,21]. Note that the exchange term of B3LYP consists of hybrid Hartree-Fock and local spin density (LSD) exchange functions with Becke's gradient correlation to LSD exchange [22]. The correlation term of B3LYP consists of the Vosko, Wilk, Nusair (VWN3) local correlation functional [23] and Lee, Yang, Parr (LYP) correlation correction functional [24]. In the present study, the normal mode analysis for each structure yielded no imaginary frequencies for the $3N-6$ vibrational degrees of freedom, where N is the number of atoms in the system. This search has indicated that the structure of each molecule considered corresponds to at least a local minimum on the potential energy surface. Furthermore, all the bond lengths have been thoroughly searched in order to find out whether any bond cleavages occurred or not during the geometry optimization process. All these computations were performed by using SPARTAN 06 program [25].

3. Results and Discussion

Aminodinitroethylene isomers, presently titled A, B and C are isoconjugates of certain alternant hydrocarbons anions (AHs) [26,27] such that isomer A is isoconjugate with a non-Kekule, whereas isomers B and C are isoconjugate with odd AHs, respectively. The isoconjugates have certain numbers of starred (n^*) and unstarred (n°) positions in their topological graphs. A non-Kekulé structure is characterized with $\Delta n \geq 2$ where $\Delta n = n^* - n^\circ$ [26,28]. By certain conformational variations or structural distortions a non-Kekule' structure may get rid of its instability.

Note that non-Kekule structures having proper explosophores are meta stable and they have the potency of an explosive such that being a non-Kekule structure is necessary but not a sufficient condition for an explosive character [29]. Many other properties are needed for a proper explosive.

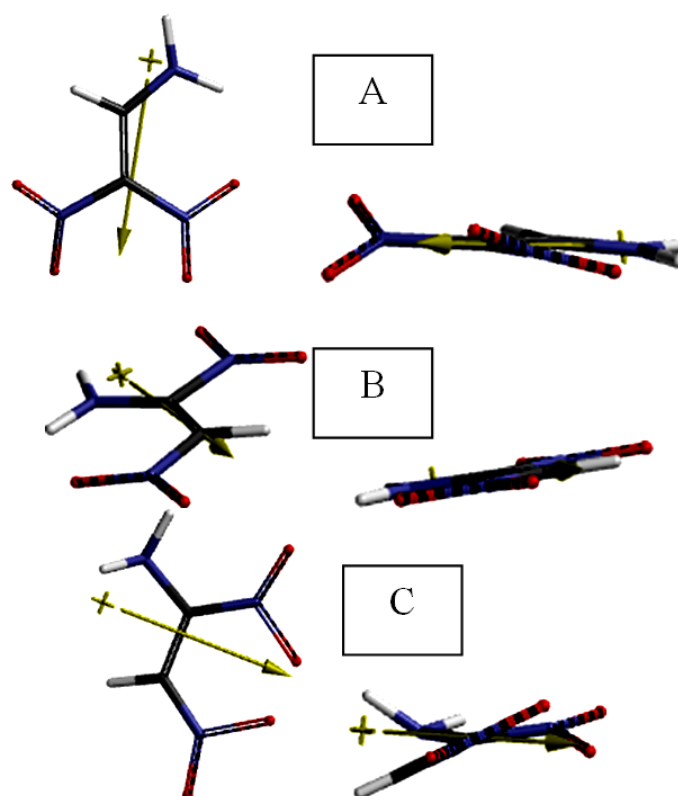


Figure 1. Optimized structures of the parent systems of consideration (Two different views).

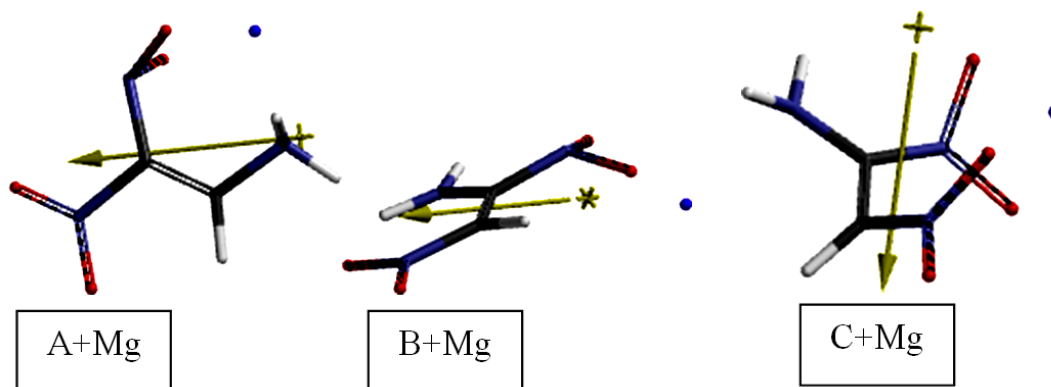


Figure 2. Optimized structures of magnesium composites of the parent structures.

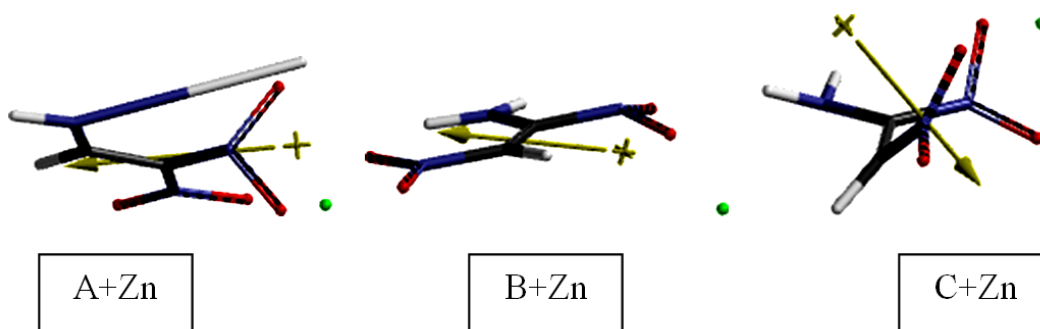


Figure 3. Optimized structures of zinc composites of the parent structures.

Optimized structures as well as the direction of dipole moment vectors of the parent aminodinitroethylenes (ADNE) are shown in Figure 1, whereas their composites with magnesium or zinc are displayed in Figures 2 and 3, respectively. The isoconjugates of aminodinitroethylenes fall into the class of alternant hydrocarbons (or anions of them).

Table 1 lists some thermo chemical properties of the species considered. Data in the table reveal that the standard heat of formation (H°) values of the species are exothermic and they are favored according to their G° (Gibbs free energy of formation) values. The algebraic orders of H° and G° values of the parent structures are $B < A < C$. Namely, the *trans* isomer is more exothermic and more favorable than the *geminal* and the *cis* isomer. The respective orders for the magnesium and zinc composites are $C+X < B+X < A+X$, where X stands for the metal component. As compared with the order for parent systems the metals have profound effect on the H° and G° values in the same direction and irrespective of the kind of the metal whether Mg or Zn.

Table 1. Some thermo chemical properties of the species considered.

Species	H°	S° (J/mol $^\circ$)	G°
A	-1425392.275	354.60	-1425498.000
B	-1425409.551	356.14	-1425515.733
C	-1425116.989	353.69	-1425222.443
A+Mg	-1950740.196	377.17	-1950852.648
B+Mg	-1950826.169	380.14	-1950939.508
C+Mg	-1950886.021	372.63	-1950997.120
A+Zn	-6096473.285	388.57	-6096589.149
B+Zn	-6096530.994	392.28	-6096647.961
C+Zn	-6096540.052	383.28	-6096654.315

Energies in kJ/mol.

Table 2 shows some energies of the species considered. Note that E, ZPE and E_C stand for the total electronic energy, zero point vibrational energy and the corrected total electronic energy, respectively [25]. The algebraic order of E_C values for the parent structures is $B < A < C$ whereas for the composites they follow the order of $C+X < B+X < A+X$, irrespective of the kind of the metal whether Mg or Zn (X stands for the metal component).

Table 2. Some energies of the species considered.

Species	E	ZPE	E_C
A	-1425599.16	198.48	-1425400.68
B	-1425614.10	196.16	-1425417.94
C	-1425318.49	192.58	-1425125.91
A+Mg	-1950941.86	195.04	-1950746.82
B+Mg	-1951029.04	196.25	-1950832.79
C+Mg	-1951089.17	196.80	-1950892.37
A+Zn	-6096633.61	191.51	-6096442.1
B+Zn	-6096695.96	195.98	-6096499.98
C+Zn	-6096703.41	194.58	-6096508.83

Energies in kJ/mol.

Figures 4-6 display the calculated bond lengths/ distances of the species considered. In the parent structures NH_2-C bonds vary in between 1.32-1.38 Å. The longest one is for the *cis* dinitro structure which indicates the relatively weak push- pull-effect present. In accordance with, the C-NO₂ bonds in structure-C are the shortest among the respective ones of the other isomers. However, one of the N-O bonds of the nitro group in C is somewhat elongated (1.51 Å). Note that it is not a completely coplanar structure.

The presence of magnesium atom does not cause any substantial structural change but the zinc atom, in structure-A causes one of the N-H bonds to cleave (4.08 Å). The zinc composites of B and C remain intact.

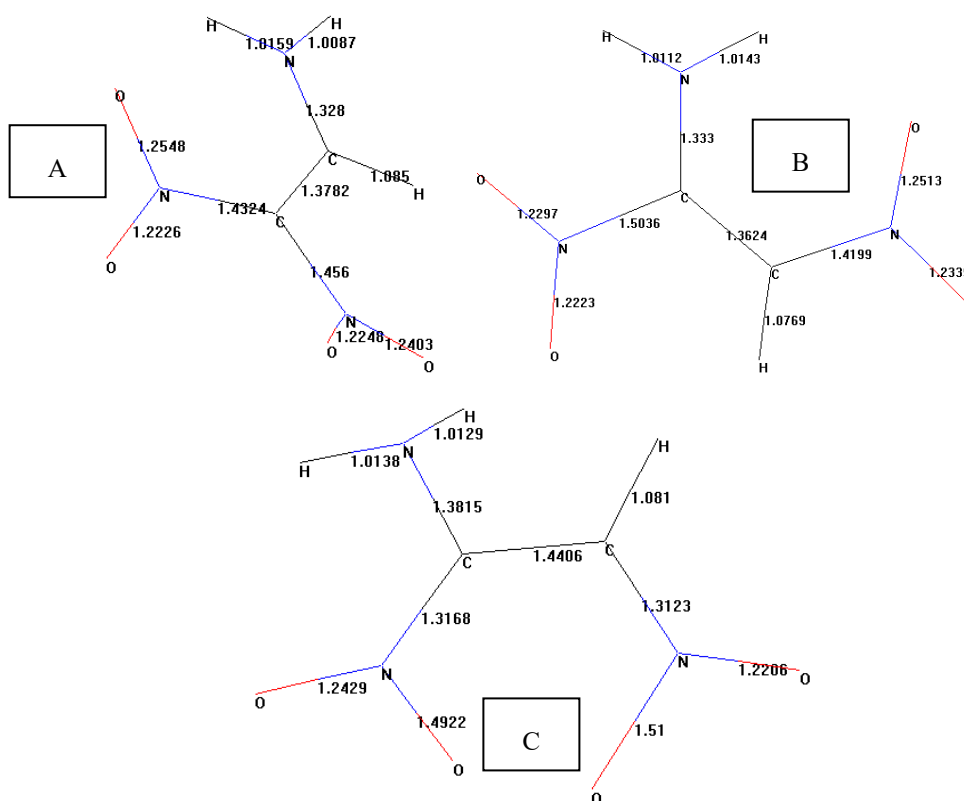


Figure 4. The calculated bond lengths of the parent structures.

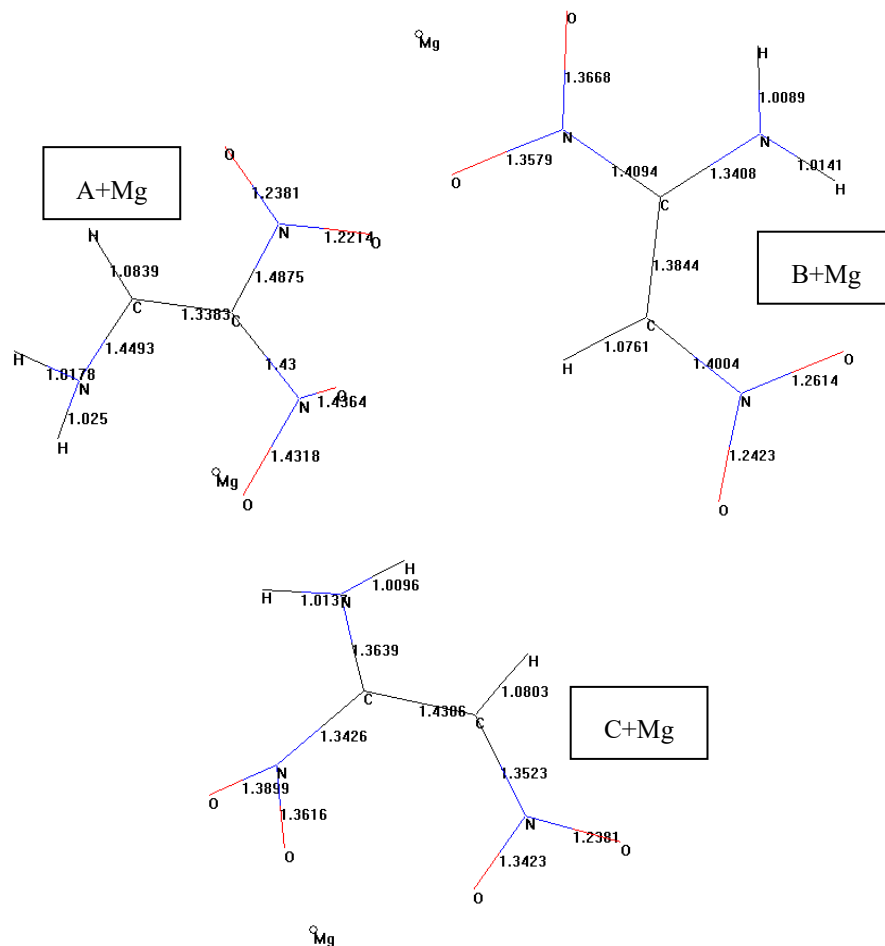


Figure 5. The calculated bond lengths of the magnesium composites of the parent structures.

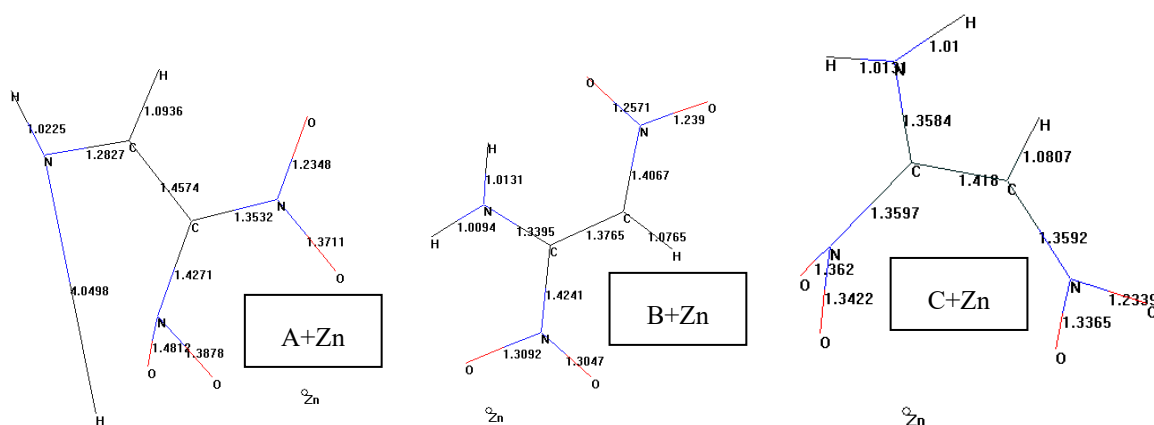


Figure 6. The calculated bond lengths of the zinc composites of the parent structures.

Figures 7-9 display electro static potential (ESP) charges on atoms of various structures presently considered. Note that the ESP charges are obtained by the program which uses a numerical method that generates charges, thus reproducing the electrostatic potential field from the entire wavefunction [25].

As seen in the figures, one common point is the NH_2 nitrogen atom possesses a negative partial charge. It is true for the parent structures as well as their composites whatever the metal components are. On the other hand, all the metal atom of the composites acquire some positive partial charge in the order of $\text{C}>\text{A}>\text{B}$ in the magnesium and $\text{A}>\text{C}>\text{B}$ in the zinc composites. So in each case the metal atom in the composites donates some

electron population to the organic component. Apparently electron demand of organic components of the composites varies depending on their structural/topological characteristics.

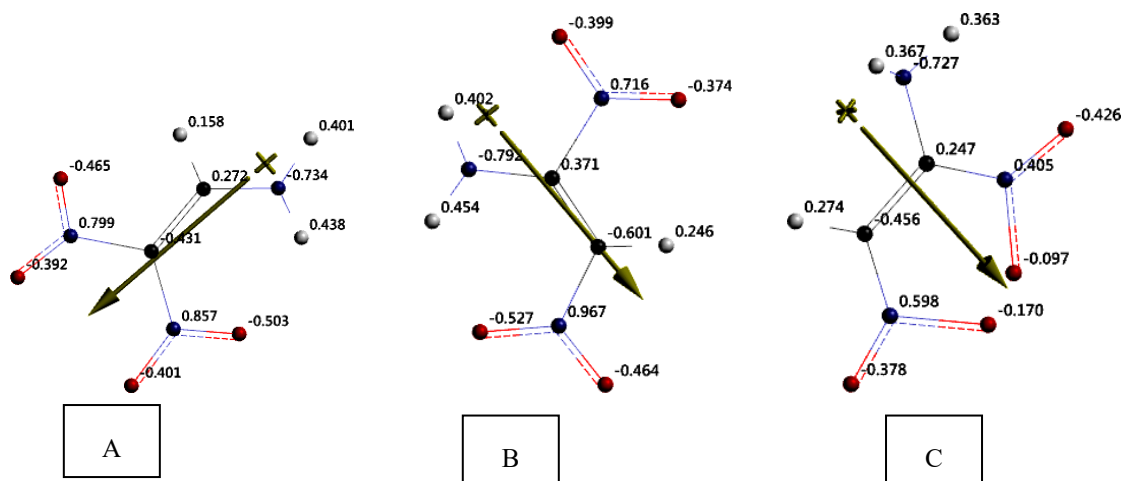


Figure 7. The ESP charges on atoms of the parent structures.

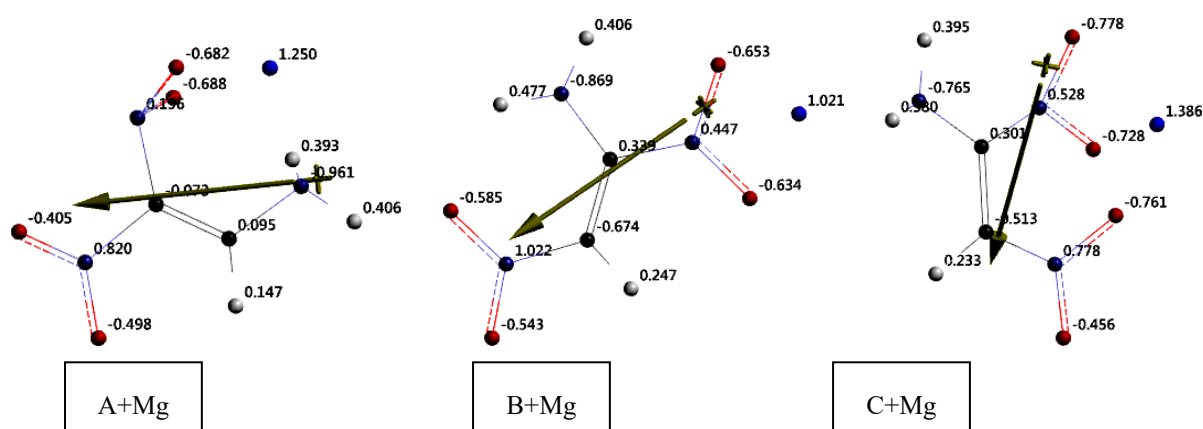


Figure 8. The ESP charges on atoms of the magnesium composites of the parent structures.

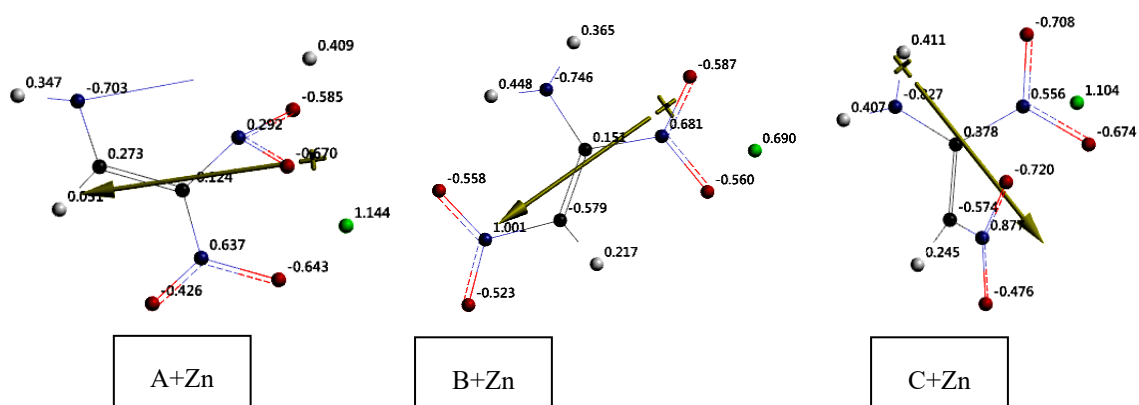


Figure 9. The ESP charges on atoms of the zinc composites of the parent structures.

Electrostatic potential maps of species are shown in Figures 10-12 where negative potential regions reside on red/reddish and positive ones on blue/bluish parts of the maps.

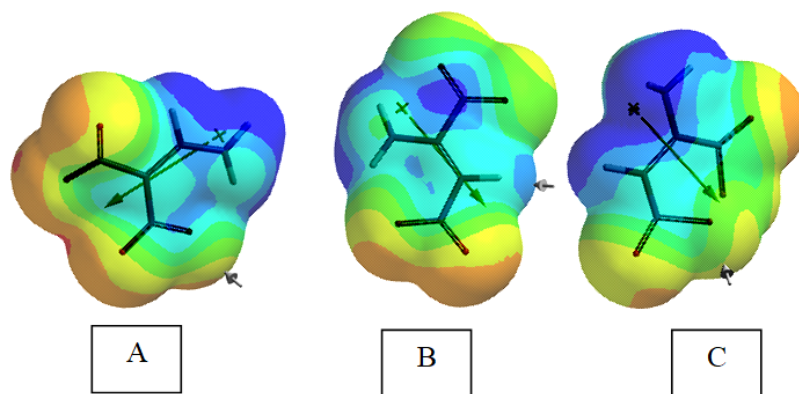


Figure 10. The electrostatic potential maps of the parent structures.

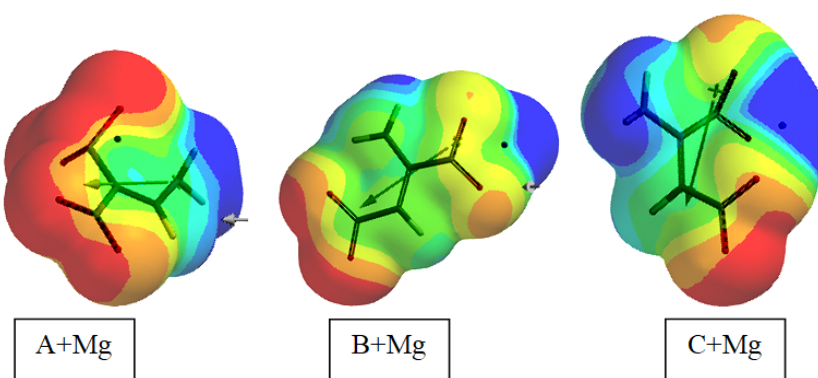


Figure 11. The electrostatic potential maps of the magnesium composites considered.

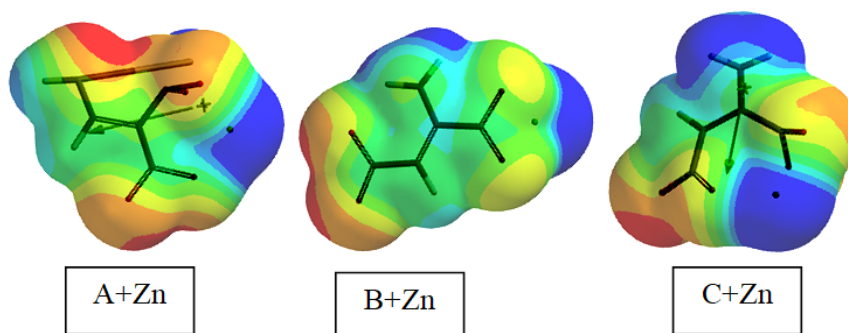


Figure 12. The electrostatic potential maps of the zinc composites considered.

Figures 13-15 display bond densities of species presently considered. As seen in the figures some unexpected electron populations exist in parent structure-C, composites A+Zn and C+Zn. In C (cis isomer), it is in between two nitro oxygens which are face to face with each other. In terms of classical approach, the nitro groups may have different group electro negativities in different positions of the molecule. Probably some intra molecular orbital interactions prevail (reminding ‘anti-electrostatic bonding between ions of like charge’ [30]). There are some evidence that in some conditions (such as colloids) like-charges attract each other [31,32]. Whereas in the zinc composites the density occurs in between the zinc atom and the organic component. Note that the zinc atom transfers some electron population and acquires some positive charge (see Figure 9). Thus, probably some bonding orbitals of the organic moiety diffuse to the positive metal. This outcome should be dictated by the over all effect of various factors.

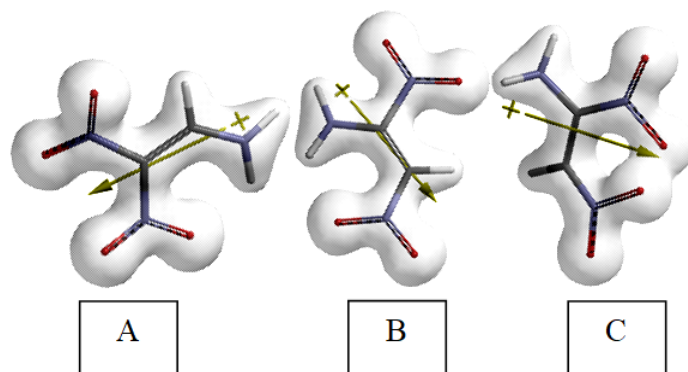


Figure 13. The bond densities of the parent structures.

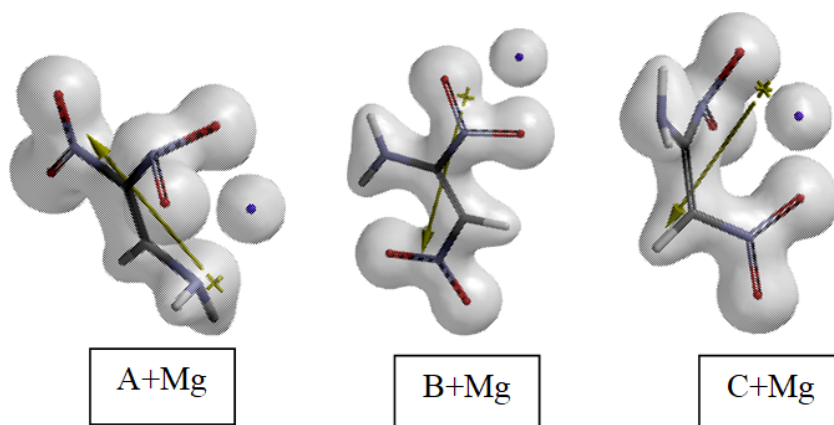


Figure 14. The bond densities of the magnesium composites considered.

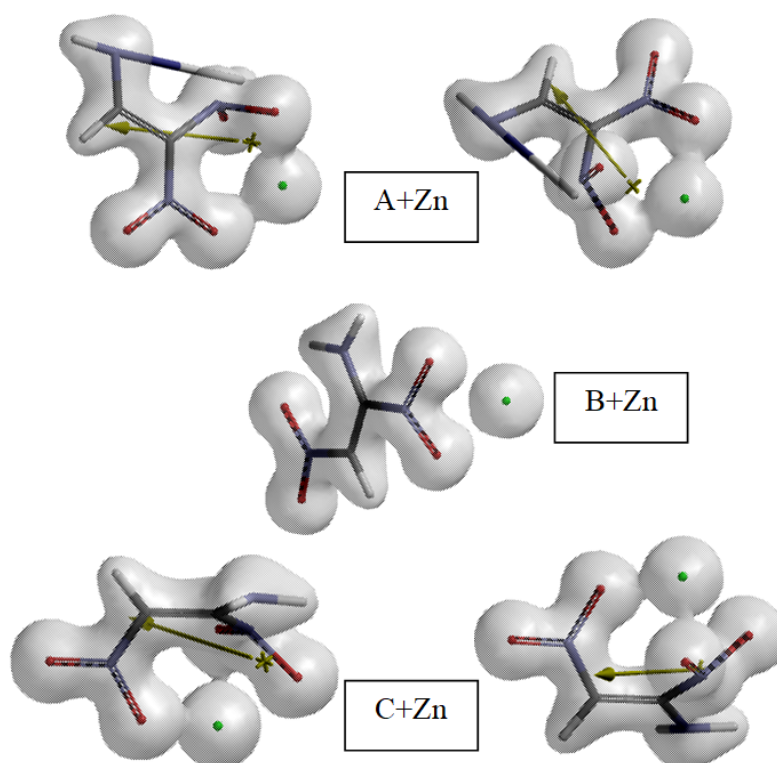


Figure 15. The bond densities of the zinc composites considered.

Local ionization potential maps of the species considered are shown in Figures 16-18 where conventionally red/reddish regions (if any exists) on the density surface indicate areas from which electron removal is relatively easy, meaning that they are subject to electrophilic attack. Note that the local ionization potential map is a graph of the value of the local ionization potential on an isodensity surface corresponding to a van der Waals surface [25].

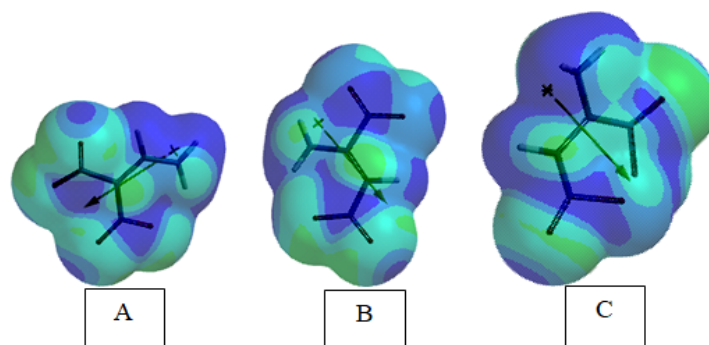


Figure 16. The local ionization potential maps of the parent structures considered.

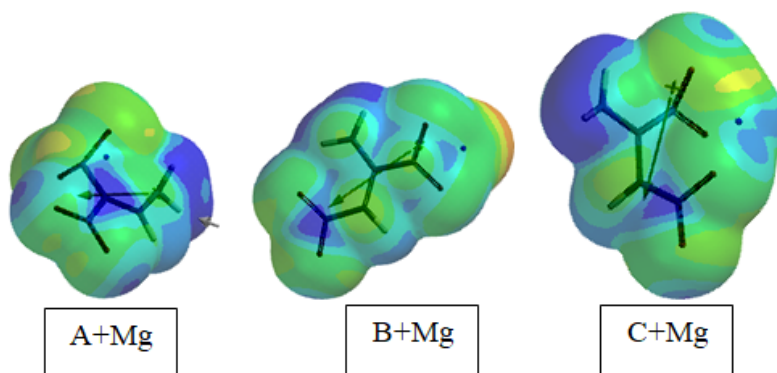


Figure 17. The local ionization potential maps of the magnesium composites considered.

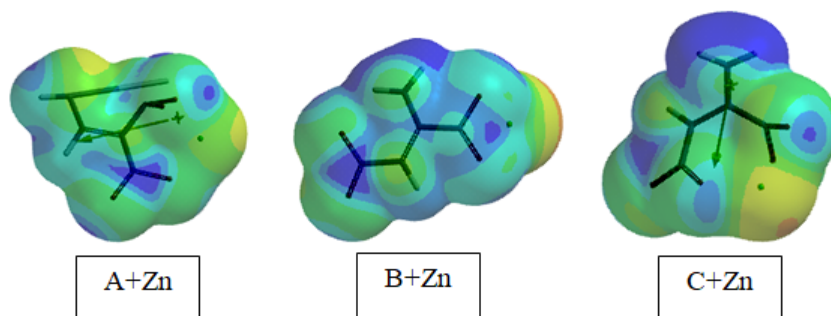


Figure 18. The local ionization potential maps of the zinc composites considered.

The LUMO maps of the species of present concern are shown in Figures 19-21. Note that a LUMO map displays the absolute value of the LUMO on the electron density surface. The blue color (if any exists) stands for the maximum value of the LUMO and the red colored region, associates with the minimum value. It is to be noted that the LUMO and NEXTLUMO (LUMO+1) are the major orbitals directing the molecule towards the attack of nucleophiles [25]. Positions where the greatest LUMO coefficient exists is the most vulnerable site in nucleophilic reactions.

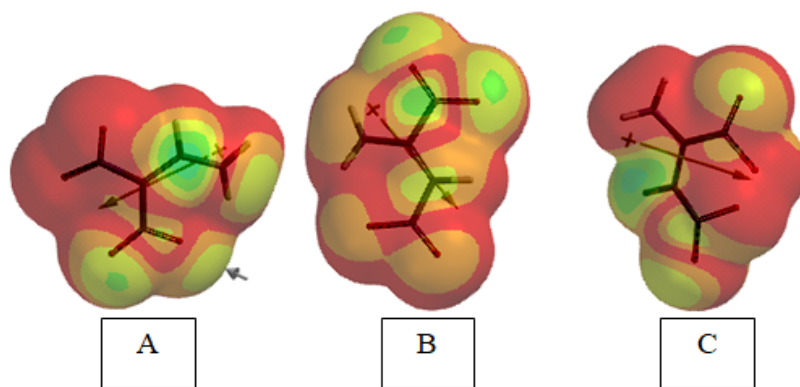


Figure 19. The LUMO maps of the parent structures.

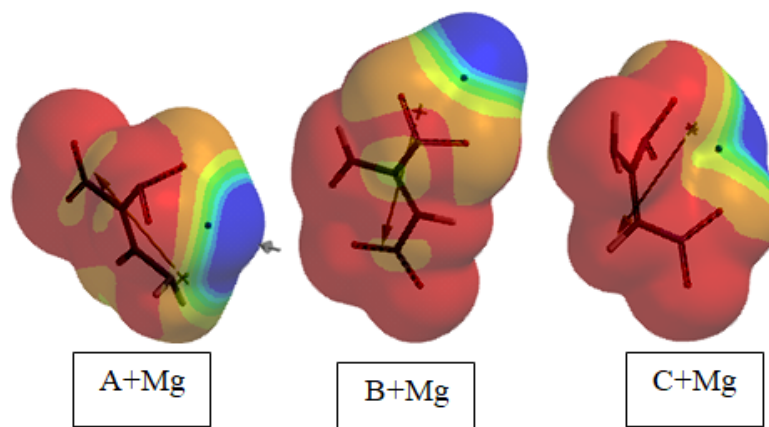


Figure 20. The LUMO maps of the magnesium composites considered.

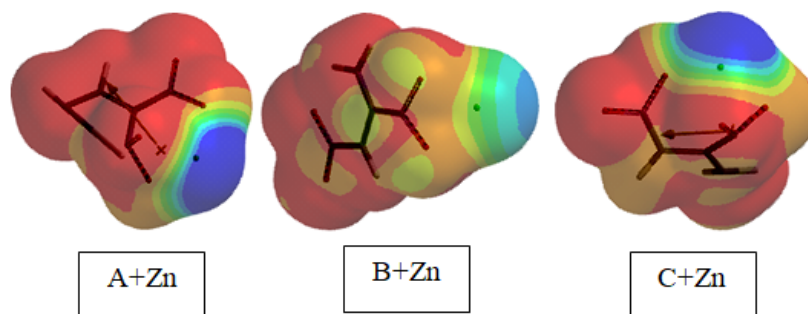


Figure 21. The LUMO maps of the zinc composites considered.

Figures 22-24 show some of the molecular orbital energy levels of structures considered.

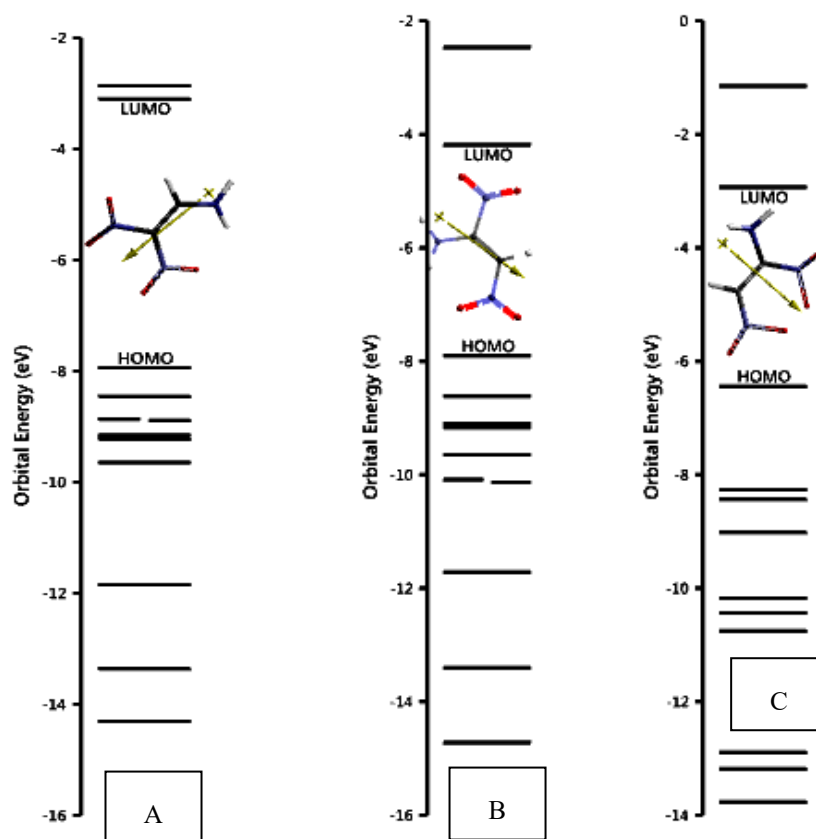


Figure 22. Some of the orbital energies of the parent structures considered.

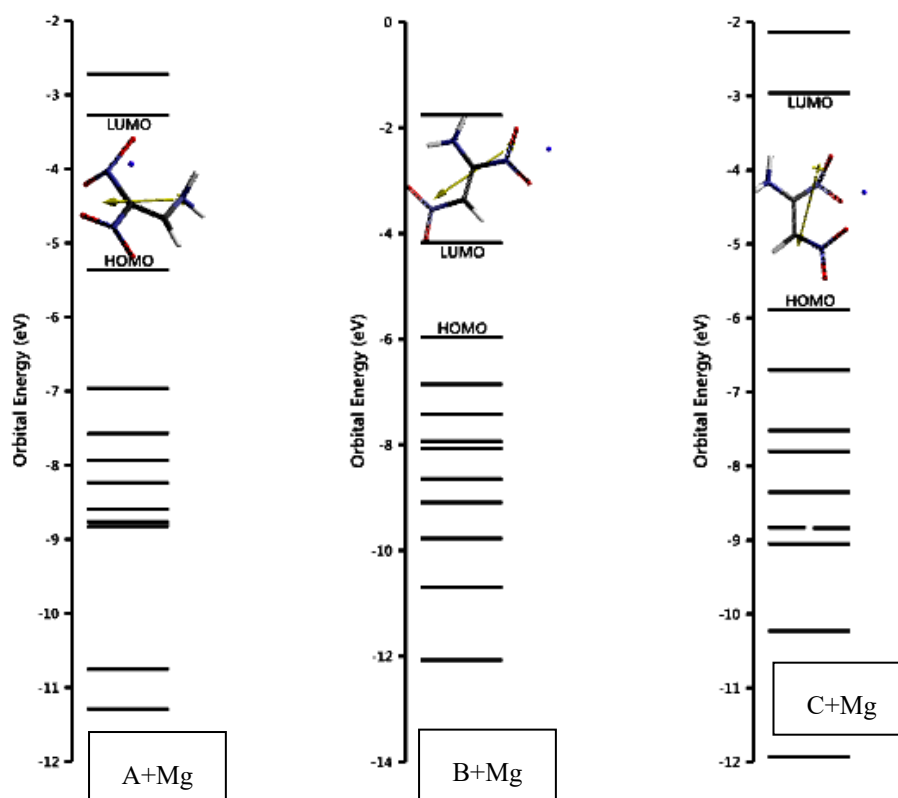


Figure 23. Some of the orbital energies of the magnesium composites considered.

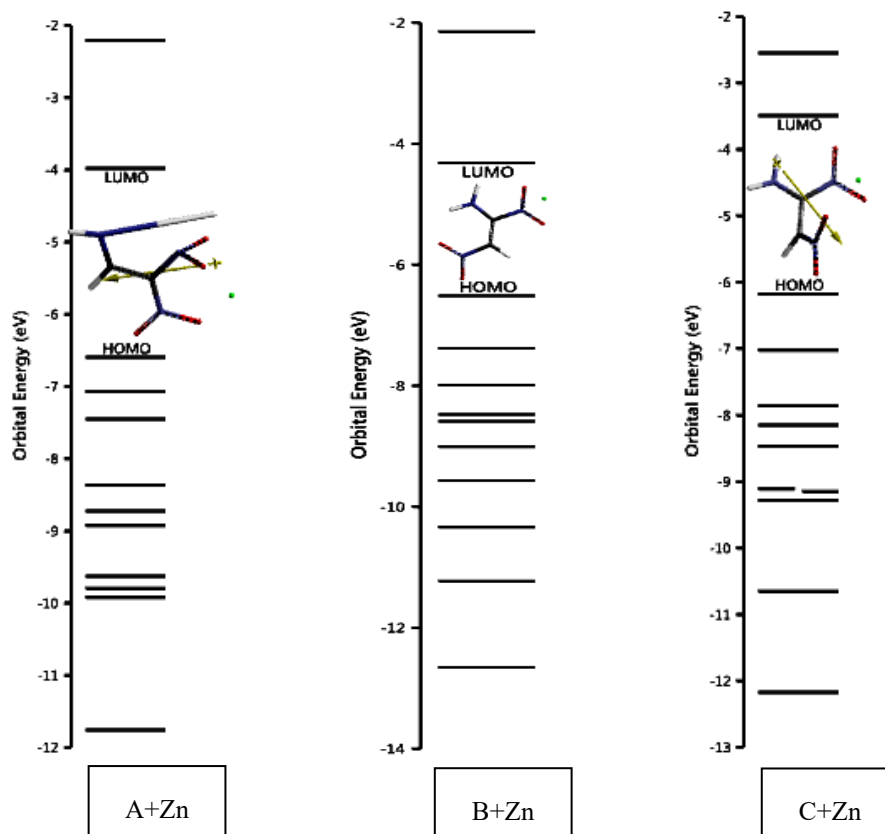


Figure 24. Some of the orbital energies of the zinc composites considered.

The HOMO and LUMO energies and the interfrontier molecular orbital gap, $\Delta\varepsilon$, values ($\Delta\varepsilon = \varepsilon_{\text{LUMO}} - \varepsilon_{\text{HOMO}}$) of the species considered are listed in Table 3. The algebraic order of HOMO and LUMO energies of the parent structures are $A < B < C$ and $B < A < C$, respectively. In the case of magnesium composites they are $B + \text{Mg} < C + \text{Mg} < A + \text{Mg}$ and $B + \text{Mg} < A + \text{Mg} < C + \text{Mg}$. Whereas, in the zinc composites $A + \text{Zn} < B + \text{Zn} < C + \text{Zn}$ and $B + \text{Zn} < A + \text{Zn} < C + \text{Zn}$, respectively. Consequently, the orders of $\Delta\varepsilon$ values for the parent and composites become $A > B > C$; $C > A > B$; and $C > A > B$, respectively.

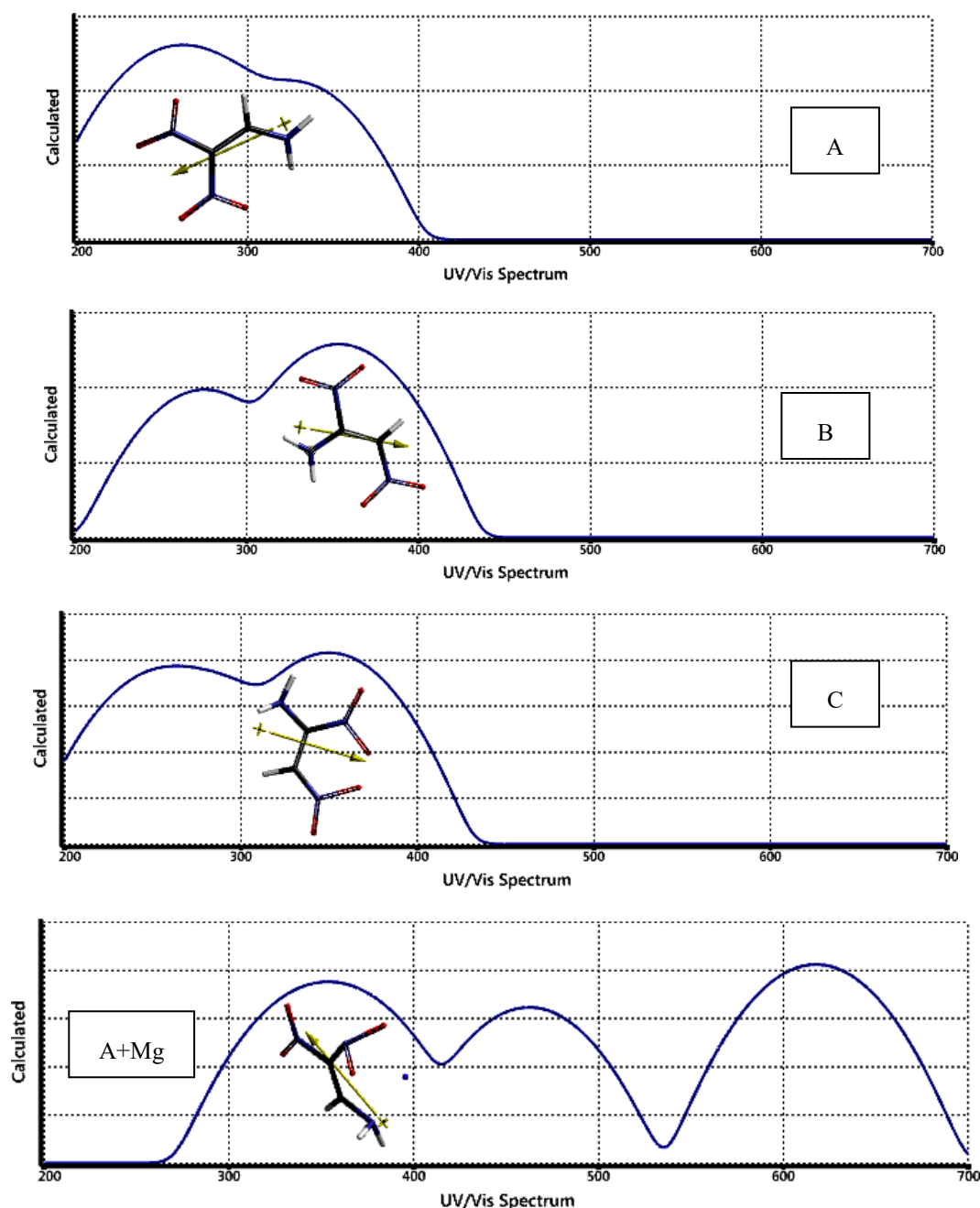
Table 3. The HOMO, LUMO energies and $\Delta\varepsilon$ values for the species of consideration.

Species	HOMO	LUMO	$\Delta\varepsilon$
A	-766.08	-298.81	467.27
B	-762.93	-403.77	359.16
C	-621.37	-283.18	338.19
A+Mg	-517.41	-315.74	201.67
B+Mg	-575.67	-402.65	173.02
C+Mg	-568.17	-285.63	282.54
A+Zn	-636.54	-383.73	252.81
B+Zn	-628.23	-416.17	212.06
C+Zn	-595.99	-336.49	259.5

Energies in kJ/mol.

Any ballistic property which correlates with the narrowness of the interfrontier energy gap ($\Delta\varepsilon$ value) should have the highest of that property value among the isomers considered. An example is the impact sensitivity, that is narrower the gap, the explosive becomes more sensitive to an impact stimulus [33-37].

Time dependent density functional UV-VIS spectra (TDDFT) [25] of some of the species of interest are shown in Figure 25. The parent structures possess the spectra mainly confined to UV region with a small skirt in the visible. Two peaks not well resolved cover the region. However, the presence of Mg atom causes appreciably striking bathochromic effect in the composites which gradually becomes less going from A+Mg to C+Mg appearing as if some hypsochromic effect has been developing.



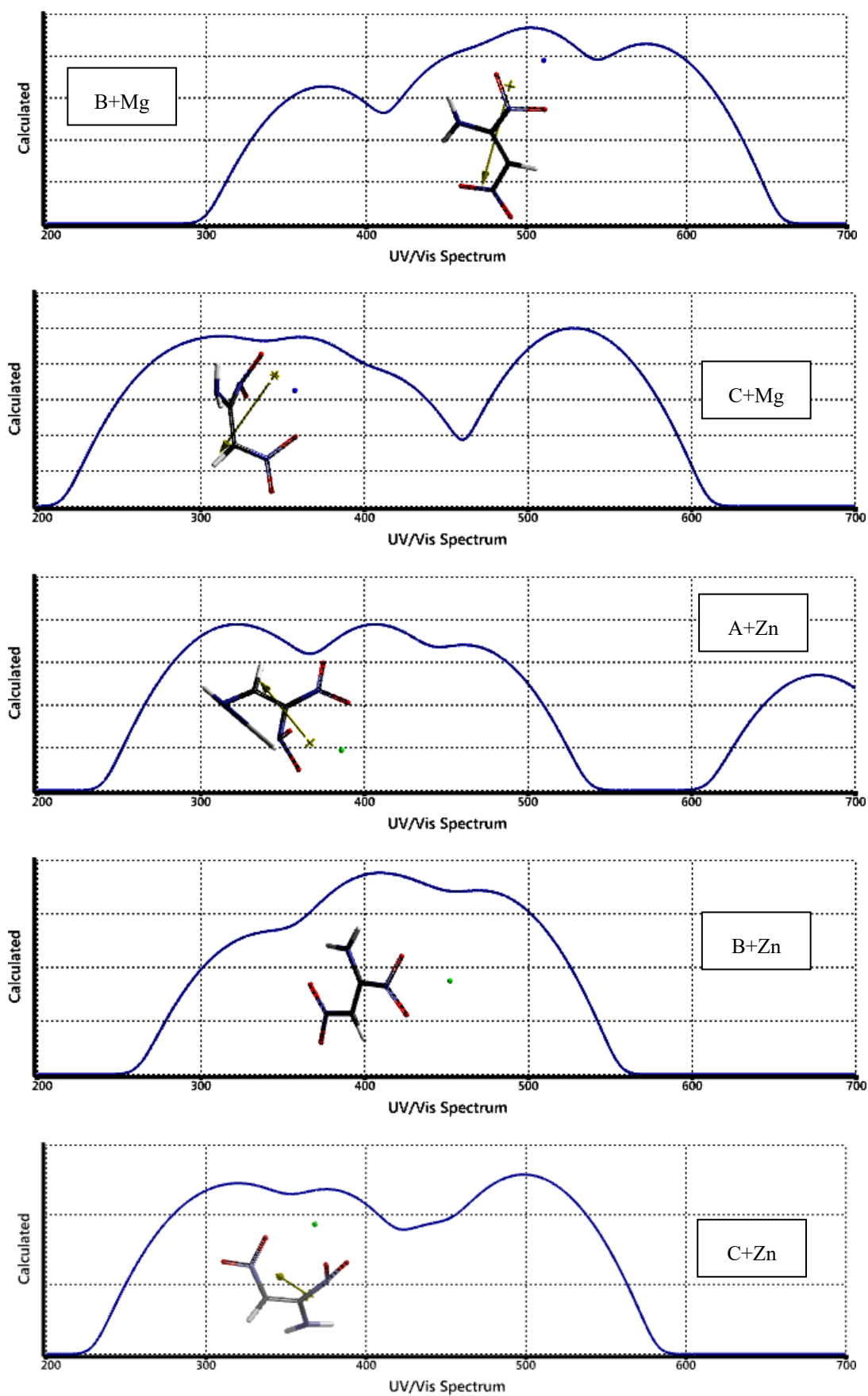


Figure 25. Time dependent density functional UV-VIS spectra (TDDFT) of some of the species of interest.

As for the zinc composites, the spectrum of A+Zn covers the whole UV and VIS region having some peaks and shoulders. Note that it is the decomposed structure by the rupture of one of the NH₂ bonds. The spectra of B+Zn and C+Zn shrink compared to spectrum of A+Zn. Note that the composites have somewhat charge-separated structures, the metal atoms have donated some electron population to the organic component, thus their spectra have been dictated by various effectors. The organic moieties of the composites under the influence of different strength of pull-push behavior (see Figures 8 and 9) which has prime importance on the UV-VIS spectra

Table 4 lists the main λ_{\max} values and intensities of the species of consideration. The calculated intensities of the peaks are related to magnitudes of the transition moments between the orbitals involved which vary from one isomeric structure to the other [4,38].

Table 4. Main λ_{\max} values and intensities of the species of consideration.

Species	
A	256.71(0.11), 287.36 (0.019), 329.05(0.011)
B	275.30(0.008), 353.42(0.144)
C	289.78 (0.013), 349.78 (0.098)
A+Mg	363.35(0.011), 462.41(0.007), 617.56(0.088)
B+Mg	369.65 (0.001), 463.48 (0.076), 503.33(0.403), 574.71(0.141)
C+Mg	293.64(0.026), 31748 (0.047), 662..83 (0.054), 528.04(0.101)
A+Zn	319.24(0.035), 406.52(0.046), 462.15(0.012), 672.12(0.001)
B+Zn	374.90(0.06), 406.26(0.394), 431.42(0.129), 472.58(0.133)
C+Zn	327.26(0.053), 376.47(0.049), 498.57(0.141)

Intensities in parenthesis.

4. Conclusion

The present computational study considered isomers of aminodinitroethylene and their magnesium and zinc composites within the restrictions of DFT at the level of B3LYP/6-31++G(d,p). Both of the isomers possess exothermic H^o and favorable G^o values. They are electronically stable. In the composites some electron population transfers from the metal to the organic components and some distortions occur. In the case of zinc composite the rupture of N-H bond of structure-A happens.

In spite of the fact that the parent structures and composites of each series are isomers of each other, the configuration and conformation of the donor and acceptor groups affect the push-pull interactions which cause various differences to arise when some properties are considered, such as UV-VIS spectra. By changing the metal to organic ratio it could be possible to get various composites having some valuable properties including the ballistic ones.

References

- [1] Agrawal, J. P. (2010). *High energy materials*. Wiley-VCH. <https://doi.org/10.1002/9783527628803>
- [2] Trzcinski, W. A., Cudziło, S., Chyłek, Z., & Szymańczyk, L. (2008). Detonation properties of 1,1-diamino-2,2-dinitroethene (DADNE). *Journal of Hazardous Materials*, 157(2-3), 605–612. <https://doi.org/10.1016/j.jhazmat.2008.01.026>
- [3] Gordon, P. F., & Gregory, P. (1987). *Organic chemistry in colour*. Springer-Verlag.
- [4] Anslyn, E. V., & Dougherty, D. A. (2006). *Modern physical organic chemistry*. University Science Books.
- [5] Ferguson, L. N. (1969). *The modern structural theory of organic chemistry*. Prentice-Hall of India.
- [6] Shvo, Y., & Shanan-Atidi, H. (1969). Internal rotation in olefins. I. Kinetic investigation by nuclear magnetic resonance. *Journal of the American Chemical Society*, 91(24), 6689–6689. <https://doi.org/10.1021/ja01052a025>
- [7] Smith, M. A., & Jasien, P. G. (1998). A CIS study of the solvent effects on the electronic absorption spectra of push-pull ethylenes. *Journal of Molecular Structure: THEOCHEM*, 429, 131–141. [https://doi.org/10.1016/S0166-1280\(97\)00346-1](https://doi.org/10.1016/S0166-1280(97)00346-1)
- [8] Carter, R. E., Dahlqvist, K. I., & Berntsson, P. (1977). N.m.r. studies of a rate process in a bridged biphenyl: Resolution of a discrepancy between n.m.r. and polarimetric kinetic data. *Organic Magnetic Resonance*, 9(1), 44–48. <https://doi.org/10.1002/mrc.1270090109>
- [9] Sandström, J., Wennerbeck, I., Nilsson, B., Enzell, C., & Matsuno, T. (1978). Studies of polarized ethylenes. Part XII. Conformational analysis of 2-dimethylamino-2-methylthio ethylenes. *Acta Chemica Scandinavica*, B32, 421–430.
- [10] Favini, G., Gamba, A., & Todeschini, R. (1985). A theoretical conformational study of push–pull ethylenes. Part 1. Substituted methyleneimidazolidines. *Journal of the Chemical Society, Perkin Transactions 2*, (7), 915–920. <https://doi.org/10.1039/P29850000915>
- [11] Lodish, H., Berk, A., Zipursky, S. L., Matsudaira, P., Baltimore, D., & Darnell, J. (2000). Noncovalent bonds. In *Molecular cell biology* (4th ed.). W. H. Freeman.
- [12] Schalley, C. A. (2012). Introduction. In *Analytical methods in supramolecular chemistry* (2nd ed.). Wiley.
- [13] Otero de la Roza, A., & DiLabio, G. A. (Eds.). (2017). *Non-covalent interactions in quantum chemistry and physics: Theory and applications*. Elsevier.
- [14] Maharramov, A. M., Mahmudov, K. T., Kopylovich, M. N., & Pombeiro, A. J. (2016). *Non-covalent interactions in the synthesis and design of new compounds*. Wiley.
- [15] Hobza, P., & Müller-Dethlefs, K. (2009). *Non-covalent interactions: Theory and experiment*. Royal Society of Chemistry.
- [16] Alkorta, I., Elguero, J., & Frontera, A. (2020). Not only hydrogen bonds: Other noncovalent interactions. *Crystals*, 10(3), 180. <https://doi.org/10.3390/cryst10030180>
- [17] Stewart, J. J. P. (1989). Optimization of parameters for semi-empirical methods I. *Journal of Computational Chemistry*, 10(2), 209–220. <https://doi.org/10.1002/jcc.540100208>
- [18] Stewart, J. J. P. (1989). Optimization of parameters for semi-empirical methods II. *Journal of Computational Chemistry*, 10(2), 221–264. <https://doi.org/10.1002/jcc.540100209>
- [19] Leach, A. R. (1997). *Molecular modeling*. Longman.
- [20] Kohn, W., & Sham, L. J. (1965). Self-consistent equations including exchange and correlation effects. *Physical Review*, 140(4A), A1133–A1138. <https://doi.org/10.1103/PhysRev.140.A1133>

- [21] Parr, R. G., & Yang, W. (1989). *Density functional theory of atoms and molecules*. Oxford University Press.
- [22] Becke, A. D. (1988). Density-functional exchange-energy approximation with correct asymptotic behavior. *Physical Review A*, 38(6), 3098–3100. <https://doi.org/10.1103/PhysRevA.38.3098>
- [23] Vosko, S. H., Wilk, L., & Nusair, M. (1980). Accurate spin-dependent electron liquid correlation energies for local spin density calculations: A critical analysis. *Canadian Journal of Physics*, 58(8), 1200–1211. <https://doi.org/10.1139/p80-159>
- [24] Lee, C., Yang, W., & Parr, R. G. (1988). Development of the Colle-Salvetti correlation energy formula into a functional of the electron density. *Physical Review B*, 37(2), 785–789. <https://doi.org/10.1103/PhysRevB.37.785>
- [25] SPARTAN 06 [Computer software]. (2006). Wavefunction Inc.
- [26] Dewar, J. M. S. (1969). *The molecular orbital theory of organic chemistry*. McGraw-Hill.
- [27] Dewar, M. J. S., & Dougherty, R. C. (1975). *The PMO theory of organic chemistry*. Plenum Press.
- [28] Dmitriev, I. S. (1981). *Molecules without chemical bonds*. Mir Publishers.
- [29] Türker, L. (2011). Recent developments in the theory of explosive materials. In T. J. Janssen (Ed.), *Explosive materials: Material science and technologies*. Nova Science Publishers.
- [30] Holthoff, J. M., Weiss, R., Rosokha, S. V., & Huber, S. M. (2021). Anti-electrostatic halogen bonding between ions of like charge. *Chemistry – A European Journal*, 27(67), 16530–16542. <https://doi.org/10.1002/chem.202102549>
- [31] Zhao, T., Zhou, J., Wang, Q., & Jena, P. (2016). Like charges attract? *The Journal of Physical Chemistry Letters*, 7(14), 2689–2695. <https://doi.org/10.1021/acs.jpcclett.6b00981>
- [32] Ball, P. (2012). Like attracts like? *Nature*. <https://doi.org/10.1038/nature.2012.10698>
- [33] Anbu, V., Vijayalakshmi, K. A., Karunathan, R., Stephen, A. D., & Nidhin, P. V. (2019). Explosives properties of high energetic trinitrophenyl nitramide molecules: A DFT and AIM analysis. *Arabian Journal of Chemistry*, 12(5), 621–632. <https://doi.org/10.1016/j.arabjc.2016.09.023>
- [34] Badders, N. R., Wei, C., Aldeeb, A. A., Rogers, W. J., & Mannan, M. S. (2006). Predicting the impact sensitivities of polynitro compounds using quantum chemical descriptors. *Journal of Energetic Materials*, 24(1), 17–33. <https://doi.org/10.1080/07370650500374326>
- [35] Zhu, W., & Xiao, H. (2010). First-principles band gap criterion for impact sensitivity of energetic crystals: A review. *Structural Chemistry*, 21, 657–665. <https://doi.org/10.1007/s11224-010-9596-8>
- [36] Zhang, H., Cheung, F., Zhao, F., & Cheng, X. L. (2009). Band gaps and the possible effect on impact sensitivity for some nitro aromatic explosive materials. *International Journal of Quantum Chemistry*, 109(7), 1547–1552. <https://doi.org/10.1002/qua.21990>
- [37] Türker, L. (2014). Interaction of TNT and aluminum – A DFT treatment. *Zeitschrift für anorganische und allgemeine Chemie*, 641(2), 408–413. <https://doi.org/10.1002/zaac.201400436>
- [38] Turro, N. J. (1991). *Modern molecular photochemistry*. University Science Books.

This is an open access article distributed under the terms of the Creative Commons Attribution License (<http://creativecommons.org/licenses/by/4.0/>), which permits unrestricted, use, distribution and reproduction in any medium, or format for any purpose, even commercially provided the work is properly cited.
